High-Viscosity Polylactide Prepared by *In Situ* Reaction of Carboxyl-Ended Polyester and Solid Epoxy

Jiuli Zhang,[1] Guan Li,[1] Yaozhen Su,[1] Rongrong Qi,[1] Dandan Ye,[1] Juan Yu,[1] Shuangwu Huang[2]

[1]*School of Chemistry and Chemical Engineering, Shanghai Jiao Tong University, Shanghai 200240, China*
[2]*Through Silicone Via Program (Dept), Institute of Microelectronics, A*STAR, Singapore 117685, Singapore*

Received 7 December 2010; accepted 23 May 2011
DOI 10.1002/app.34951
Published online 1 September 2011 in Wiley Online Library (wileyonlinelibrary.com).

ABSTRACT: To extend the potential applications of polylactide (PLA) in film blowing, foaming, thermal molding, and so on, the high-viscosity PLA composites with various compositions of carboxyl-ended polyester (CP) and solid epoxy (SE) have been successfully prepared by an *in situ* reaction blending process. Their rheological properties, crystallization behaviors, tensile properties, and morphologies have been investigated in detail. The results show that the complex viscosity η^*, G', and G'' at low-frequency region and the tensile strength of PLA composites are obviously improved with the addition of CP/SE, but the nonisothermal crystallization of PLA component is hindered. SEM reveals that some microphase separations existed in the as-prepared composites. © 2011 Wiley Periodicals, Inc. J Appl Polym Sci 123: 2996–3006, 2012

Key words: polylactide; carboxyl-ended polyester; solid epoxy

INTRODUCTION

Nowadays, the use of traditional plastics from fossil resources is under scrutiny because of their nonbiodegradable nature and the increasingly environmental consciousness. Fortunately, the industrial and research communities have discovered or created a family of durable degradable plastics as the replacement for petroleum-derived plastics. Among them, biodegradable polyesters inclusive of polylactide (PLA), poly(ε-caprolactone) (PCL), poly(butylenesuccinate), poly(glycolic-acid), and poly(3-hydroxybutyrate)[1,2] have attracted great research interests in environmental, medical, and pharmaceutical applications. Their degradation mechanisms are usually attributed to a simple hydrolytic process, in which ester bonds react with water and then break down to form carboxyl and hydroxyl terminal groups.

As a kind of linear aliphatic polyesters synthesized by the ring-opening polymerization of lactides, PLA is typically derived from corn starch fermentation,[1] and has good mechanical properties, thermal plasticity, biocompatibility, and ease of fabrication.[2] These characteristics enable PLA as a promising polymer for various applications.[3] Another feature of PLA is the good safety upon exposure to heat. For example, it does not produce any toxic nitrogen oxide gases and only one third of the combustible heat of polyolefins is generated when it is burned, so it does not damage the incinerator and provides significant energy savings.[4] However, the instable processability of PLA needs to be concerned, that is, thermo-oxidative, hydrolytic degradations, and so on. The instability of PLA usually leads to break the polymer chains, as a result to decrease its molecular weight.[5] And it would further result in a deterioration of rheological properties, which should be avoided for a processing purpose, especially when high levels of melt viscosity and strength are required. For example, the viscosity and strength of material has significant influence on their final performance when they are in blow molding, blow film, extrusion, and foaming.

As is well known, PLA has a very low viscosity and melt strength, so the fabricated films are far away from stability and close to rupturing during blow-film process; and the lower melt tension is not beneficial to obtain satisfying products during blow-molding process. To overcome such shortcomings, attempts to improve the melt rheological properties of PLA have motivated considerable research efforts. One of the most important techniques is increasing the molecular weight of PLA, which can efficiently improve the intrinsic melt intensity of PLA. However, the productivity would decrease for high molecular PLA because of the prolonged reaction time, and the degradation or the color changing is usually inevitable. Furthermore, some investigations on the free radical branching/crosslinking of PLA has been

Correspondence to: R. Qi (rrqi@sjtu.edu.cn).
Contract grant sponsor: Shanghai Leading Academic Discipline Project; contract grant number: B202

also carried out in the melt mixing process in an extruder or in a kneader with the presence of trace amounts of various peroxides (served as radical initiators).[6–8] In these process, branching or crosslinking reaction of PLA molecule chain can happen to some extent because of the reaction of capturing hydrogen by peroxides. However, some of new problems would appear because of the high reactivity of peroxides, such as the excessive crosslinking reaction and the degradation of PLA, which is hard to avoid during such processing. Another method is incorporating some new functional groups onto the PLA backbone to improve its melt viscosity, which paves the way to prepare composites, coated items, and composites/alloys. For example, multi-isocyanate[9] and multi-epoxide[10] are often used to endow PLA functional groups through copolymerizing reactions during reactive extrusion process, but a good knowledge on the reaction and control of polymerization during manufacturing are necessary. However, the copolymerization reaction is often difficult to realize anticipative results because of the difference of reactive activity between lactide and copolymerizing ester, and the melt intensity of PLA can be seldom improved. Therefore, extensive investigations on polymer blend technology have been also carried out. Blending PLA with another immiscible or miscible polymer with higher melt viscosity is perhaps a less expensive and practical alternative way to prepare a variety of useful composites and alloys. Blends of PLA with PCL,[11,12] atactic poly[(*R*, *S*)-3-hydroxybutyrate],[13] poly(ethylene succinate),[14] hydrophilic poly(vinyl alcohol),[15] poly(methyl methacrylate),[16] poly(ethylene glycol),[17] and poly(vinylphenol),[18] have been investigated. Most of the above studies revealed that blending PLA with other polymers can substantially modify the mechanical and thermal properties, degradation rate, and permeability, but few distinct evidence of the improvement for melt viscosity can be found in these blends. Recently, Jiang et al.[19] showed that the melt elasticity of the biodegradable PLA/poly(butylene adipate-*co*-terephthalate) blends increased with the concentration of PBAT increasing via blending process, but the viscosity increase is limited.

Carboxyl-ended polyester (CP) and solid epoxy (SE) have been widely used in polyester powder coating because they can form a crosslinking structure, and the viscosity of PLA will increase after *in situ* crosslink if CP and SE are added into the PLA matrix. In this article, CP and SE are used as the modifier of PLA to improve the melt rheological properties of PLA. Compared with the above-mentioned methods (increasing molecular weight, branching/crosslinking and incorporating new functional groups into PLA backbone), this method with CP/SE as the modifier has some outstanding advantages. For instance, the reaction temperature of CP/SE is close to the processing temperature of PLA; CP/SE has a high melt viscosity after reaction, and abundant functional end groups, which are easily accessible. With the unique crosslinking structure after reaction, CP/SE results in the different dispersion phase size and stereo hindrance for the linear polymer. Furthermore, the abundance of hydroxyl end groups attached to CS/SE may have some H-bonding interactions with PLA.[20] Thus, it is reasonable to expect that the incorporation of CP/SE into PLA may bring about either the improved melt viscosity or the increased strength.

Based on the above consideration, this study attempts to prepare PLA/CP/SE composites via so-called *in situ* reaction method to improve the melt viscosity of PLA. The high viscosity of the composites can be easily realized by reactive extrusion and compression molding. The rheological, thermal, tensile properties, crystalline, and morphology were also studied in detail.

EXPERIMENTAL

Materials

PLA (3051D, melt flow rate (210°C, 2.16 kg) of 25 g/10 min, specific gravity of 1.25 g/cm^3) was purchased from Natureworks LLC., Houston, TX. CP (P5980, M_w = 3000 g/mol by gel permeation chromatography) and SE (E903, epoxy equivalent = 700 g/mol by technical parameters) were kindly supplied by DSM, Heerlen, Holland. Antioxidant 1010 and 168 were purchased from Ciba Specialty Chemicals, Shanghai, China.

Preparation of composites

To keep samples dry sufficiently, the dry condition of the samples (PLA, CP, and SE) are setting according to Sudduth's works and given as following[21]: PLA pellets were dried under vacuum at 60°C for 12 h before being used; CP and SE powders were previously dried under vacuum at 50°C for 12 h before melt blending. Then PLA, CP and SE were simultaneously introduced into the twin-screw extruder (Berstorff, Hannover, Germany) after dry blending. The extrusion temperature was independently controlled on eight zones along the extruder barrel and a strand die to achieve a temperature profile ranging from 80 to 165°C at screw speed of 120 rpm. After exiting from the die, the extrudant was granulated by a pelletizer. The obtained pellets were further dried at 60°C in a vacuum oven for 24 h before the compression molding.

The as-obtained pellets were compressed into flat sheets with 1 or 3 mm thickness on our laboratory

TABLE I
The Results of Distilling Experiment About PLA/SE Composites

PLA/SE	99/1	97/3	95/5	90/10	80/20
M_0/g	2.625	2.745	2.856	2.842	2.767
M/g	0.084	0.148	0.175	0.203	0.187
$C_{PLA\text{-}SE\text{-}PLA}$/%	3.20	5.39	6.13	7.14	6.76

compression-molding machine at 180°C under 16 MPa for 10 min and subsequently cooled at room temperature for 15 min.

Measurement

The content of PLA-SE

To study the reaction between expoxy and PLA, the pellets (SE series, seen in Table I) were extracted by refluxing hot acetone for 72 h to remove the un-reactive PLA and SE, and then dried to a constant weight in a vacuum oven. Measure the initial weight (M_0) and the extracted weight (M), and the content of PLA-SE-PLA ($C_{PLA\text{-}SE\text{-}PLA}$) is calculated by the formulation (1).

$$C_{PLA-SE-PLA} = M/M_0 \times 100\% \quad (1)$$

Fourier transform infrared (FTIR)

The obtained samples were compressed into the film (1–1.5 μm) for FTIR characterization. IR spectroscopy information was obtained on a Perkin–Elmer Paragon 1000 Fourier transform infrared spectrophotometer (PerkinElmer, Waltham, MA).

Rheological properties

For the study of rheological behaviors, the samples were pressed into 1 mm thick plates at 180°C. The rheological measurement was carried out on a Gemini 200 Rheometer instrument (Bolin Instruments, East Brunswick, NJ). Frequency sweep for the samples was carried out under nitrogen at 190°C using 25 mm plate-plate geometry, and the sample gap was set as 0.5 mm. A strain sweep test was initially conducted to determine the linear viscoelastic region of the materials. The strain and angular frequency range used during testing were 5% and 0.01–100 rad/s, respectively. Gemini 200 software was used to acquire the data.

DSC

Thermal analysis was carried out on a DSC from PerkinElmer, Waltham, MA, model DSC-7. Approximately 5–10 mg of each blend was weighted and sealed in an aluminum pan. First, a sample was heated from 20 to 200°C at a ramp rate of 100°C/min and held isothermally for 3 min, and then cooled to 20°C at the cooling rate of 10°C/min (first scan). After that, the sample was reheated from 20 to 200°C at a heating rate of 10°C/min (second scan). The glass transition temperature (T_g) was taken as the midpoint of the heat capacity change. The cold crystallization peak temperature (T_{cc}) was determined from the DSC exotherm, whereas the melting temperature (T_m) and the enthalpy of fusion (ΔH_m) were determined from the DSC endotherm. The crystallinity of PLA (X_c) was calculated by means of the following equation:

$$X_c(\%) = \frac{\Delta H_m - \Delta H_c}{w\Delta H_m^0} 100\%, \quad (2)$$

where ΔH_m and ΔH_c are the experimental melting enthalpy and cold crystallization enthalpy of PLA crystals, respectively, and w is the weight fraction of PLA in the composites. A value of $\Delta H^0{}_m = 106$ J/g was used according to a reported enthalpy of melting of 100% crystalline PLA.[22]

POM

Polarized optical microscope (POM, LEICA-DMLP1, Leica Microsystems GmbH, Wetzlar, Germany) was used to study the crystallization morphology of the specimens. The specimens were first heated to 200°C and kept for 3 min. Then the specimens were cooled from the melt to the selected crystallization temperature at 120°C with a rapid cooling rate. The PLA spherulites were observed after isothermal crystallization for 30 min.

SEM

Scanning electron microscopy (SEM) *S*-2150 from Hitachi, Tokyo, Japan was used to characterize the fracture surface of compress-molded samples.

Tensile properties

Tensile tests were carried out on Instron 4465 (Instron Corp, Norwood, MA) machine according to the ASTM D790 test method using dumb-bell-shaped samples punched out from the molded films. The tensile speed was 10 mm/min, at 23°C under 50% relative humidity. At least five specimens were tested for each sample to get an average value.

RESULTS AND DISCUSSION

Reaction of CP/SE with PLA

Because of multifunctional end groups of CP and SE, they can readily carry out crosslinking reaction

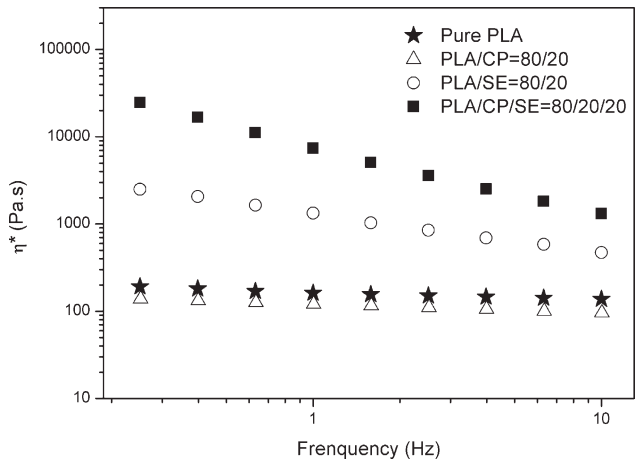

Figure 1 Comparison of η* of pure PLA, PLA/CP, PLA/SE, and PLA/CP/SE.

and/or form hydrogen bonding with PLA to increase its melt viscosity. However, the similar processing temperature also makes the synthesis simpler. Therefore, CP and SE were used as the modifiers to improve the properties of PLA in this study.

After CP, SE, and PLA were blended at high temperature, three main chemical reactions were perhaps happened: (a) Reaction between CP and SE; (b) Ester-ester interchange between PLA and CP;[23] (c) Reaction between PLA and SE. To study the possible reactions among them, the viscosity of different samples (pure PLA, PLA/CP blend, PLA/SE blend, and PLA/CP/SE blend) has been compared, and the results are given in Figure 1. From Figure 1, one can see that the viscosity of PLA/CP blend is slightly lower than that of pure PLA, while the viscosity of PLA/SE and PLA/CP/SE is much higher than that of pure PLA, and the viscosity of PLA/CP/SE is the highest. According to the works of Sudduth[23] and Mondragon and Nazabal,[24] large drop in melt viscosity could usually be obtained when transesterification was happened in blends comparing to that of two dry blend polyesters normally. While PLA/CP blend prepared in the present work has only slightly lower viscosity than that of pure PLA, indicating the reaction between PLA and CP could be negligible. In general, typical ester–ester interchange reactions in blends usually happened at 290°C for ~ 18 min, or at 250°C for about 36 min.[24] However, the processing temperature in our work was 180°C, at which ester–ester interchange would be extremely slow or nearly negligible.[25] The slight decrease of viscosity of PLA may be attributed to the low viscosity of low molecular weight CP. However, the increase of viscosity for PLA/SE and PLA/CP/SE composites may be attributed to the reaction between CP/SE or PLA/SE. Because CP/SE can significantly increase the viscosity of PLA, PLA/CP/SE will be used in the following works.

Scheme 1 shows the possible chemical reactions of PLA/SE/CP composites, such as the mainly crosslinking of CP/SE (I),[26,27] the side reactions between SE and PLA (II) and some potential interaction with PLA such as the hydrogen bonding (III). From Scheme 1, it is expected that the crosslinking reaction of CP and SE might generate the stereo hindrance for the linear polymer and thus increase the viscosity of PLA. Furthermore, the as-formed abundant hydroxyl groups have the potential to interact further with PLA, most likely via hydrogen bonding. Thus, it is quite expectable that the incorporation of CP/SE into PLA may improve the melt rheological properties of PLA. Furthermore, some controlled experiments, including the ratio of CP to SE, process temperature and process control, were also designed to investigate their effects on the viscosity of final blends. According to the suggestion of DSM Co., different experiment conditions and results are shown in Scheme 2, in which the ratio of CP : SE is fixed to 1 : 1 by weight. In other words, the crosslink between CP and SE has been completed after compression molding at 180°C under 16 MPa for 10 min.

Meanwhile, the possible side reactions between SE and PLA may occur because of the high reactive activity of epoxy group. These side reactions could also affect the reactive efficiency of CP and SE, change the composites into more complicated, and further increase the viscosity of the system.

We tried to prove directly the reaction among CP, SE, and PLA by FTIR, but the spectrum is too complex to be identified. So PLA/SE composites have been prepared to prove the reaction between SE and PLA. Through the weight change of PLA/SE composites before and after extraction, the reaction between SE and PLA has been investigated. The results are given in Table I. From Table I, it can be seen that the $C_{PLA\text{-}SE\text{-}PLA}$ increases with the increase of SE content, indicating the reaction between PLA and SE. Figure 2 also presents the FTIR spectra of pure PLA, pristine SE and PLA-SE-PLA (after extraction). Several characteristic bands of PLA are located at 754 and 872 cm^{-1} (C—H bend); 1045–1211cm^{-1} (C—O stretch); 1456 cm^{1} (CH_3 bend); 1750 cm^{-1} (C=O stretch, ester group); 2945 cm^{-1} (CH stretch); 2997 cm^{-1} (CH_3 stretch); and 3510 cm^{-1} (OH stretch, end group).[28] The main bands in the IR spectrum of SE can also be detected: a broad band at around 3510 cm^{-1} (OH stretch); a strong overlapped band at 3100–2900 cm^{-1} (CH_3 stretch); two bands at 1380 and 1330 cm^{-1} (CH_3—C—CH_3 stretch); a strong band at 1260 cm^{-1} (C—O); 1300–1100 cm^{-1} (C—O—C); a band at 913 cm^{-1} (epoxy group); and 645 cm^{-1} (phenyl group). Compared with the characteristic bands of PLA and SE, some

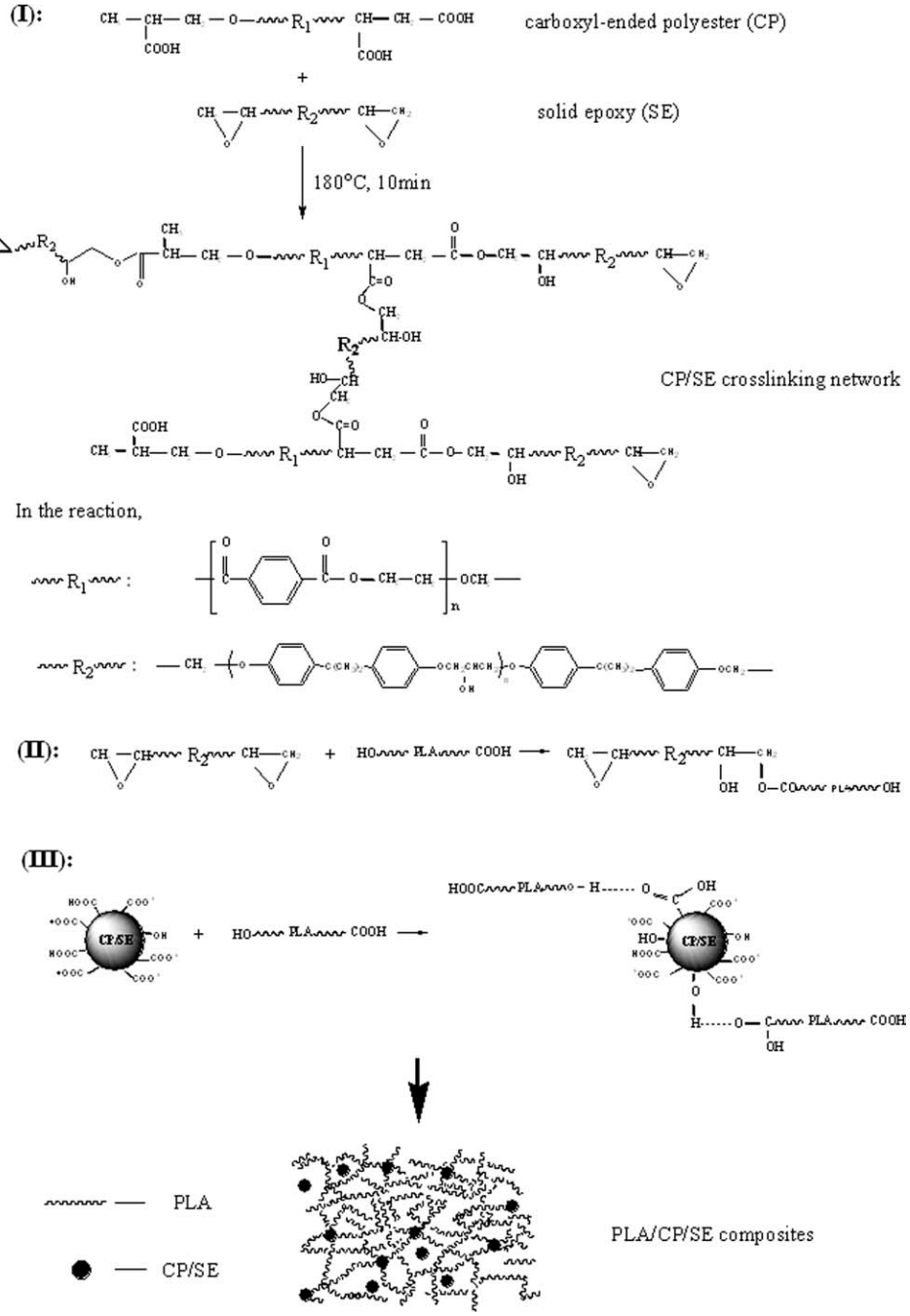

Scheme 1 The preparation of PLA/CP/SE composites.

noticeable changes occur in the spectrum of PLA-SE-PLA. For example, an original strong band of PLA at 1750 cm^{-1} for the ester group becomes weaker and marked wider; the bands of SE at 3100–2900 cm^{-1} for CH_3 appeared and a overlapped band at around 3510 cm^{-1} for OH shift lower wavenumber 3464 cm^{-1}, indicating that part of the intramolecular hydrogen bond converting to intermolecular interactions, while the band at 913 cm^{-1} for epoxy disappears. Moreover, the viscosity of PLA/SE composites is higher than that of pure PLA. The above results imply that expoxy participates in the reaction and generates ester in PLA/SE composites.

Rheological behavior

PLA/CP/SE composites with different proportion have been prepared, and the detailed formulation is given in Table II. Compared with pure PLA, no casting can be observed and the extrudant bar is not easy to break, implying the obtained composites have good mobility and can be reformed by extrusion, injection,

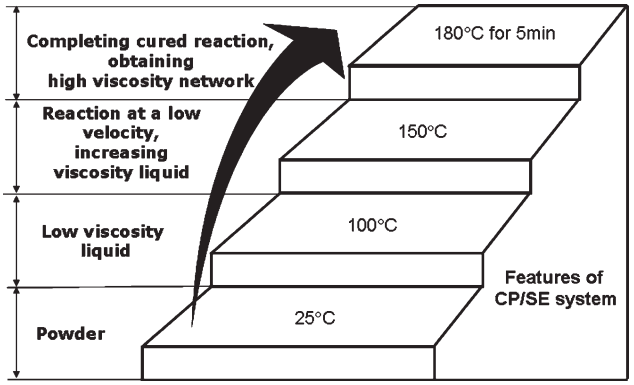

Scheme 2 The reactive conditions of CP and SE.

and compression molding. To determine the effect of CP/SE network on the viscosity of PLA, the melting rheological property has been studied. The complex viscosity (η*)-frequency curves for PLA and its composites are shown in Figure 3.

From Figure 3, one can see that the complex viscosity of PLA/CP/SE composites have a significant increase (over two orders of magnitude) when the loading of CP and SE is higher than 5%. In general, the complex viscosity (η*) is mainly dependent on the frequency region studied. At low-frequency region, PLA and its composites with low level of CP and SE (<3%) exhibit an obvious Newtonian behavior of the melt. However, such Newtonian behavior could not be observed as the loading of CP/SE increasing (Fig. 3). In contrast, all the samples show similar viscous behavior at high-frequency region, indicating the improved sensitivity to frequency. This phenomenon is probably associated with the structural change of PLA via the crosslinked CP/SE network strengthening the copious entanglements and steric hindrance of PLA linear chains when CP/SE is incorporated into PLA matrix. Furthermore, the free volume usually plays a major role in the internal friction forces experienced by the units involved in motion. With the decrease of free volume, the internal friction of molecules increases, which would lead to the melt viscosity increase markedly. Therefore, the free volume will become smaller with the addition of CP/SE because their abundant hydroxyl groups could form hydrogen bonding with the carboxylic groups of PLA.[29] Thus, the replacement of a certain amount of PLA by CP/SE in this work can obviously increase the complex viscosity of PLA, especially at low-frequency region, which could realize the expectation of blow-film, blow-molding, and foaming into full play.

TABLE II
The Formulations for PLA/CP/SE Composites

Samples	PLA (phr)	CP (phr)	SE (phr)	1010 (phr)	168 (phr)
PLA	100	0	0	0.5	0.5
99/1/1	99	1	1	0.5	0.5
97/3/3	97	3	3	0.5	0.5
95/5/5	95	5	5	0.5	0.5
90/10/10	90	10	10	0.5	0.5
80/20/20	80	20	20	0.5	0.5

It is well-known that the complex viscosity can be separated into the two parts-the storage modulus G' and the loss modulus G''.[30] The elastic part of the complex melt viscosity is represented by G', while the viscous part is described by G''. Plotting G' and G'' against frequency are given in Figure 4. From Figure 4, one can see that they have similar increasing trend as that for η*, and both of them monotonically increase with the increase of CP/SE content at all frequencies. If the polymer chains are fully relaxed, they would exhibit characteristic terminal behavior [i.e., G' (ω^2) and G'' (ω)].[31] As can be concluded that the slope of G' or G'' versus ω in the log-log plot for pure PLA is 1.09 or 0.96 at low-frequency region after fitting curves. As the slope of G' deviates from the homopolymer-like terminal slope

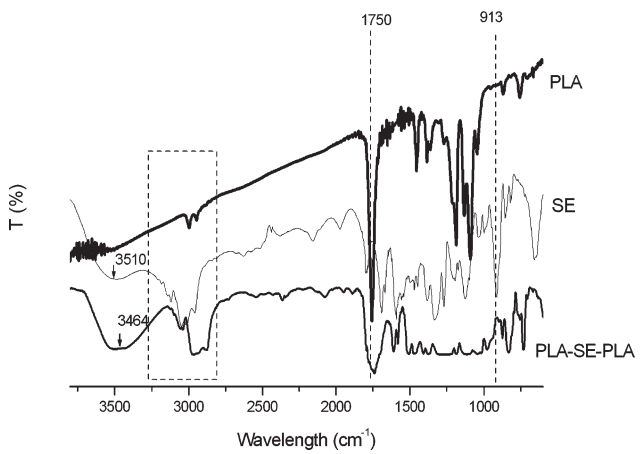

Figure 2 FTIR spectra of PLA, Epoxy, and PLA-Epoxy.

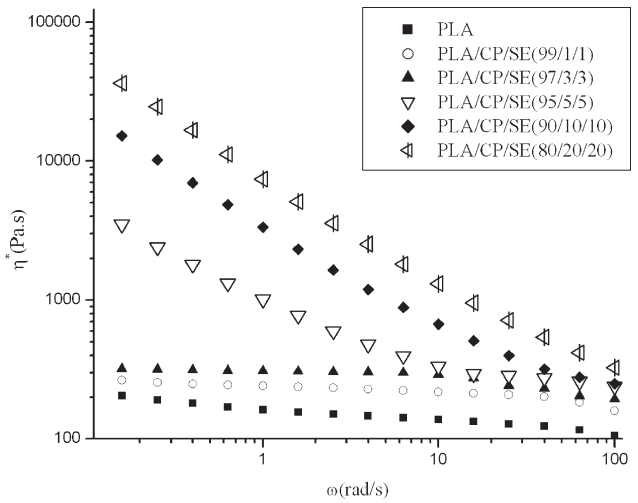

Figure 3 η* of PLA and PLA/CP/SE composites.

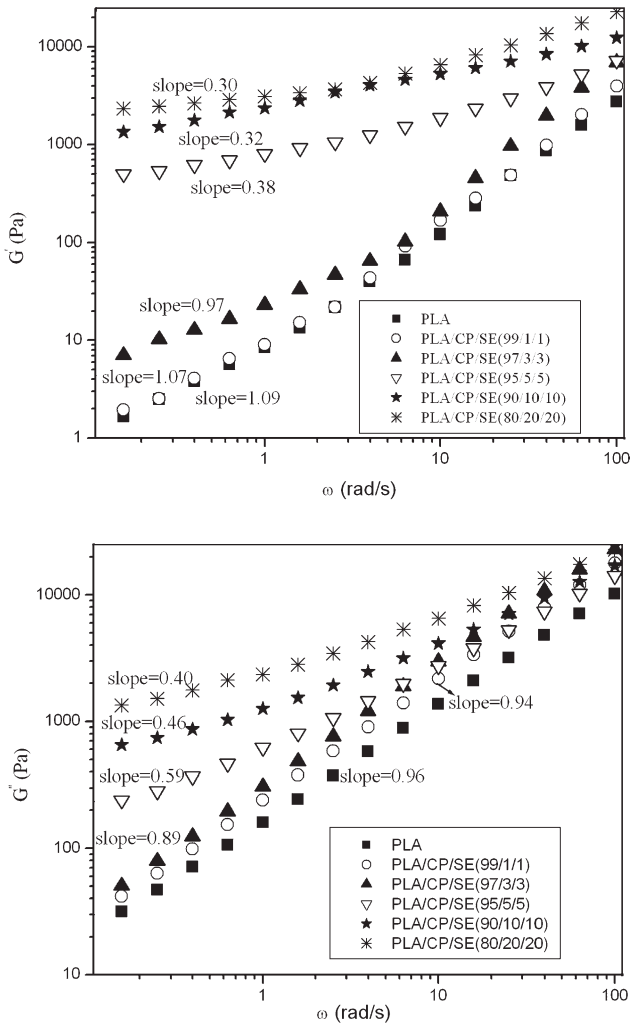

Figure 4 G' and G'' of PLA and PLA/CP/SE composites.

(2.0) of the monodispersed linear polymer, this phenomenon indicates the polydispersity of PLA molecular weight. While the slopes for the PLA/CP/SE composites decreases with the increase of CP/SE load, which may be relate to the compatibility of composites.[32] The decrease of the slope for G' and G'' may imply the incompatibility of dispersed phase and matrix. Therefore, PLA/CP/SE composites may be in microphase-separated structure. And the frequency dependence of G' and G'' in the phase separation region may be attributed to composition fluctuations and the presence of dispersed phase. Meanwhile the observed change in the slope of G' and G'' may be also caused by phase-separation, which will be further discussed in DSC and SEM analysis.

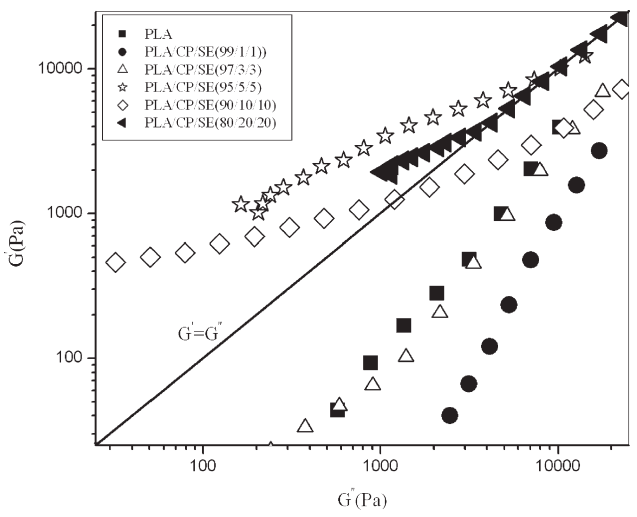

Figure 5 G' versus G'' of PLA and PLA/CP/SE composites.

To better understand the viscoelastic properties of PLA/CP/SE composites, a Cole–Cole plot is useful for comparing the differences in these properties at low-frequency region, which can be well seen from a plot of G' versus G'' (Fig. 5) (the Cole–Cole plot).

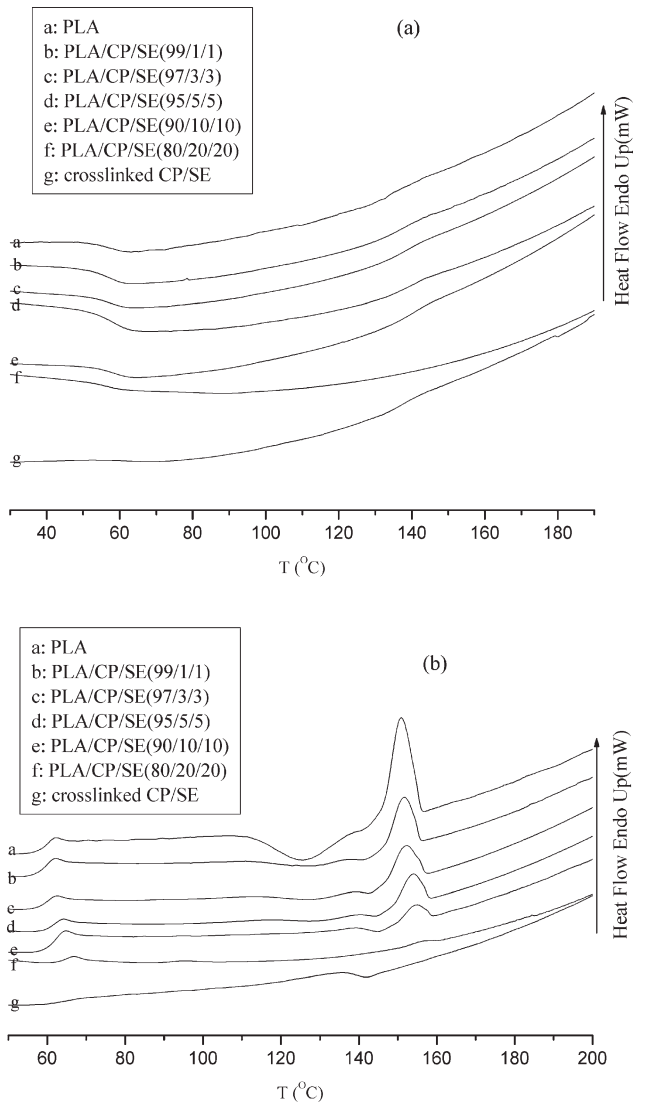

Figure 6 DSC curves of PLA, CPSE, and PLA/CP/SE composites: (a) First scan DSC thermogram at a cooling rate of 10°C/min; (b) Second scan DSC thermogram at a heating rate of 10°C/min.

TABLE III
Thermal Properties of the PLA and Its Composites (Second Scan)

PLA/CP/SE composites	$T_{g,PLA}$ (°C)	$T_{cc,PLA}$ (J/g)	$\Delta H_{c,PLA}$ (°C)	$T_{m,PLA}$ (°C)	$\Delta H_{m,PLA}$ (J/g)	$\chi_{c,PLA}$ (%)
100/0/0	60.2	126.0	5.04	151.3	19.58	13.72
99/1/1	60.8	128.2	1.04	152.1	9.33	7.98
97/3/3	62.3	130.1	0.72	152.3	6.93	6.22
95/5/5	63.6	131.0	0.45	152.2	5.47	5.23
90/10/10	64.6			153.1	2.12	
80/20/20	65.2			154.0	0.51	

The intersection ($G' = G''$) determines the transition from more viscous behavior ($G' < G''$) to more elastic behavior ($G' > G''$). Although PLA and all composites exhibit both viscous and elastic behavior at 190°C, the elastic part increases in the composites with increasing CP/SE (more than 5%) content, especially at low-frequency region. The result also explains the network formation of CP/SE and the intermolecular interaction between PLA and CP/SE in another way, that is, hydrogen bonding and the chemical reaction between carboxyl and epoxy.

Thermal performance

To investigate the compatibility of PLA and CP/SE, thermal performance of the composites was studied by DSC (Fig. 6). The presence of sluggish exothermal peaks in Figure 6(a) and sharp peaks in Figure 6(b) indicates that both the pure PLA and its composites are in the semicrystalline state with the T_g value at about 60°C and the melting peak at about 151°C, while the crosslinked CP/SE is an amorphous polymer with the T_g at about 140°C. In the PLA/CP/SE composites, there are two glass transitions indicating their microphase-separation. Moreover, one can observe that the T_g of PLA/CP/SE slightly increases with the increase of CP/SE content [Fig. 6(b)], which also illustrates that PLA and CP/SE are partially compatible due to the weak molecular interaction, that is, hydrogen bonding may exist between PLA and CP/SE in spite of the presence of microphase-separation in the obtained composites.

Crystallization behavior

The cold crystallization behavior of all composites at the second heating stage has been investigated, and

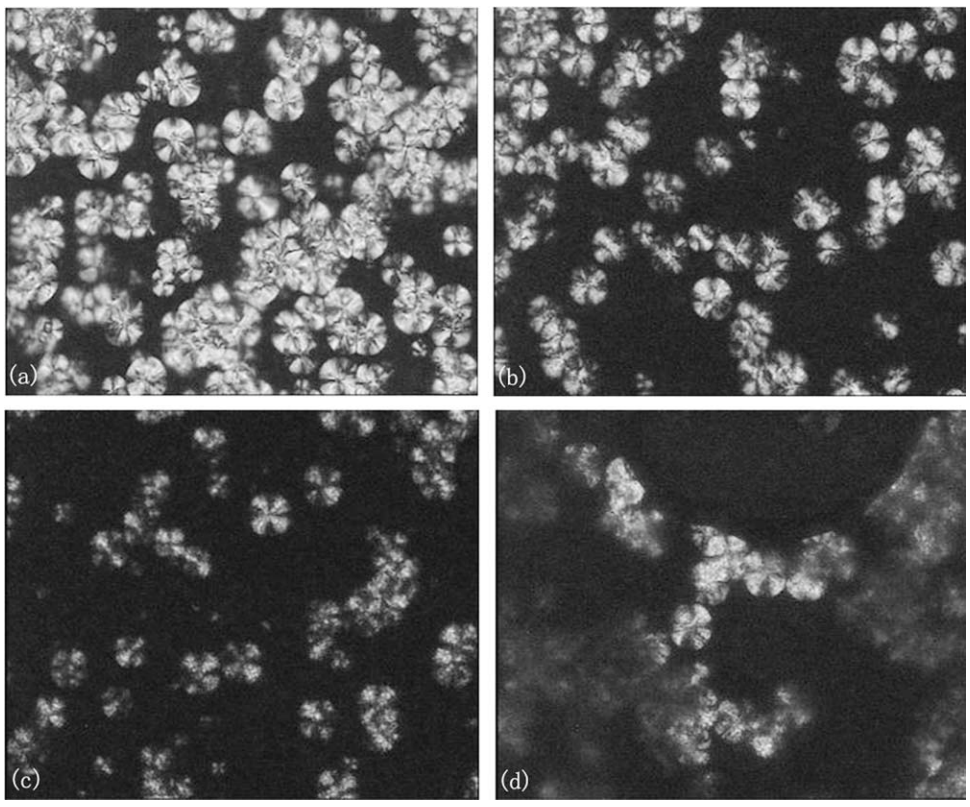

Figure 7 Polarized optical microscopy images of neat PLA(a) and PLA/CP/SE composites of (b) 99/1/1, (c) 95/5/5, and (d) 90/10/10 after isothermal crystallization at 120°C for 30 min.

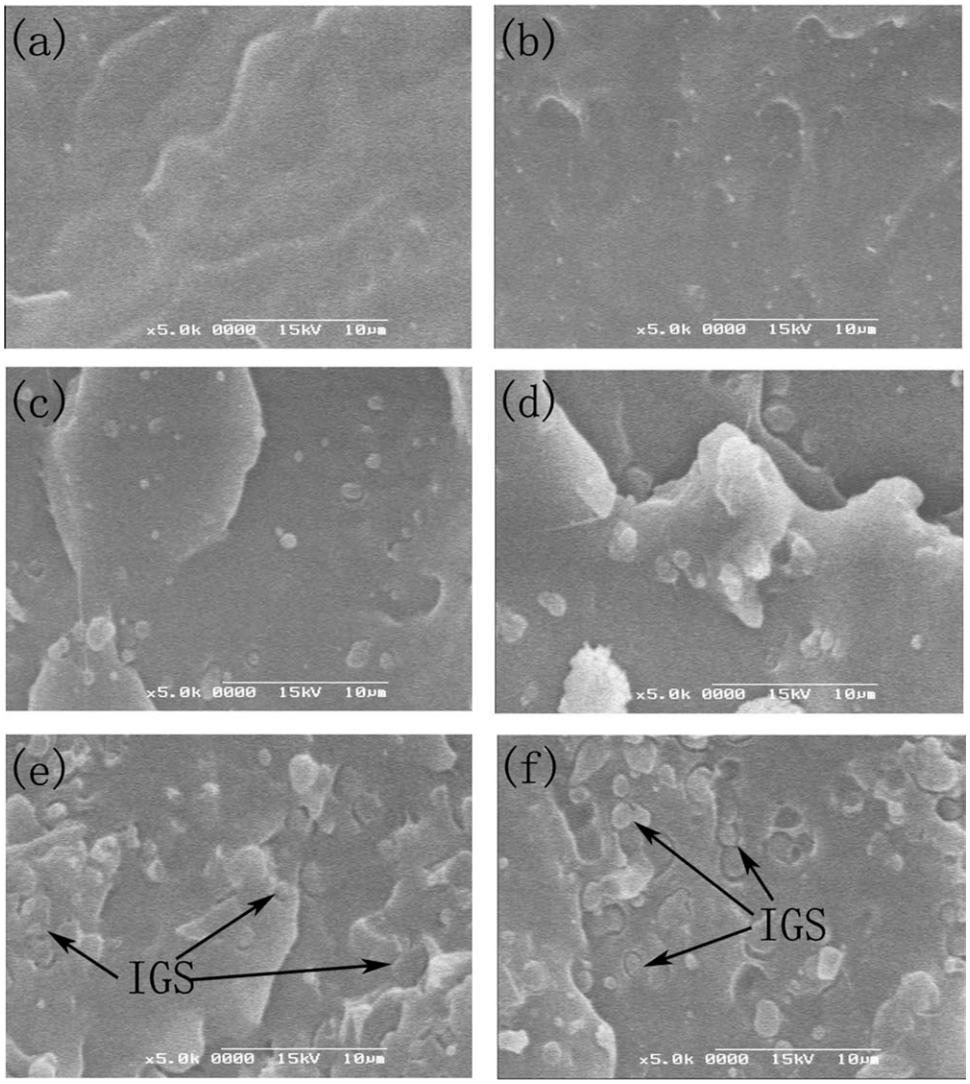

Figure 8 SEM images of PLA and its composites PLA/CP/SE: (a) 100/0/0, (b) 99/1/1, (c) 97/3/3, (d) 95/5/5, (e) 90/10/10, and (f) 80/20/20.

the results are given in Figure 6(b) and summarized in Table III. Nearly constant T_m of PLA can be observed for all samples, suggesting no change of the crystal structure of PLA/CP/SE composites. However, the influence of CP/SE on crystallization behavior of PLA still exists. Pure PLA represents a tiny broad exothermic peak at 126°C, indicating a rather low cold crystallization capability.[17] However, this peak becomes weaker and merely appears at higher temperature, or even disappears at high CP/SE content in PLA/CP/SE composites. Meanwhile, the heat of cold-crystallization (ΔH_c), the heat of melting (ΔH_m) and degree of crystallinity (χ_c) of PLA decreases continuously upon increasing CP/SE content in Table 3. These results indicate that the incorporation of CP/SE can significantly weaken the crystalline ability of PLA. Just as stated earlier, the incorporation of CP/SE network can result in more entanglements and smaller free volume of PLA chains compared with pure PLA, further hinder the mobility of PLA segment, and thus weaken the crystalline ability of PLA.

The simultaneous crystallization phenomenon was further confirmed by the polarized optical micrographs under crossed polarizer (Fig. 7). The temperature ramp profiles were same to that in the DSC scan, and the samples were isothermally crystallized at 120°C for 30 min. From POM images (Fig. 7), numerous spherulites are noticed which can be ascribed to the interaction of crystallized PLA and amorphous CP/SE. In addition, both pure PLA and its composites show typical spherulites with a Maltese Cross despite of the CP/SE content. In pure PLA, the spherulites are almost completely full of the bulk and affect each other, indicating that large amount of PLA crystal nucleus are formed and they easily grow during the crystallization process. However, the nucleus density of crystallites distinctly

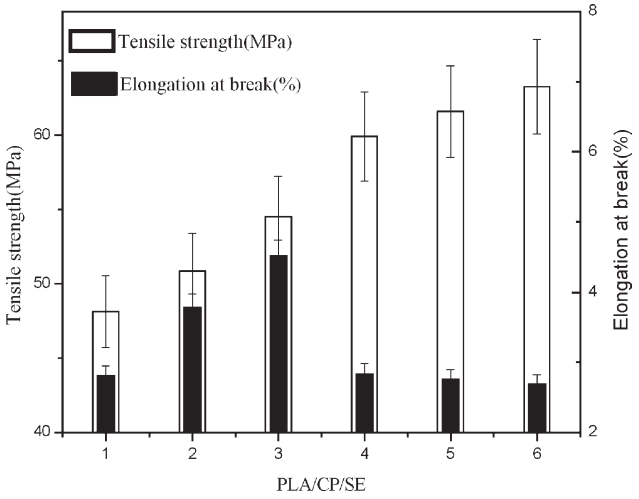

Figure 9 Tensile properties of PLA and PLA/CP/SE composites: (1) 100/0/0, (2) 99/1/1, (3) 97/3/3, (4) 95/5/5, (5) 90/10/10, and (6) 80/20/20.

decreases with the increase of CP/SE content, and the PLA crystals become vague and irregular and lack of typical Maltese Cross. These further indicate that CP/SE can hinder the crystal growth of PLA.

Morphology

The fracture surfaces of pure PLA and its composites were observed using SEM (shown in Fig. 8). A typical brittle breakage can be observed on the fracture surface of pure PLA [Fig. 8(a)]. In Figure 8(b–f), microphase separation with vague interface due to the partially compatibility of PLA and CP/SE can be observed in all PLA/CP/SE composites, and the second phase has spherical geometry and is well dispersed in the matrix. This microphase-separated structure of the composites is in agreement with the T_g and T_m obtained from the DSC measurements. Inoue et al. has proposed that the spinodal phase-separation induced by chemical reaction is observed in an epoxy/polyethersulphone system having a lower critical solution temperature type phase diagram.[33,34] Reaction-induced spinodal phase-separation yields a variety of two-phase structures: interconnected globule structures [IGS, as confirmed in Fig. 8(e,f)], and isolated domain structures with uniform domain size [as confirmed in Fig. 8(b–f)], and which depends on the competitive rates of the chemical reaction and the phase separation. The formation of the interconnected-globule structure may experience as follows: the crosslinking structure of the epoxy resin forms through *in situ* curing after the temperature reaches the curing temperature, and results in the sudden increase of the molecular weight of the epoxy resin leading to a phase separation. However, if a network is preformed in the epoxy-rich region, a complete interruption cannot be realized and this eventually results in the interconnected-globule structure.

Tensile properties

For the purpose of the ultimate applications of materials, mechanical properties were also investigated. The tensile properties of PLA and its composites are shown in Figure 9. Pure PLA is rigid and brittle with the elongation at break of 2.8%. With the increase of CP/SE content, the tensile strength of the composites increases, while the elongation at break initially increases and then slightly decreases. As to the improvement of tensile properties, CP/SE plays an important role because of the *in situ* forming crosslinked network, especially the interconnected globule structures. Moreover, the molecular interaction between PLA and CP/SE also has some effects, that is, the reaction between carboxyl in PLA and epoxy in SE, and hydrogen bonding. However, the crosslinked network of CP/SE can also hinder the movement of molecular chain of PLA leading to the decrease of the elongation at break.

CONCLUSIONS

The high-viscosity PLA/CP/SE composites were successfully prepared *in situ* reaction blending, which indicates that CP/SE can effectively improve the viscosity of PLA. Their rheological properties, crystallization behavior, morphology, and tensile properties were affected to different extents by the incorporation of CP/SE components. The important results were summarized following:

1. There are some interaction between PLA and SE, and which results in the partially compatibility of PLA/SE/CP.
2. The addition of CP/SE can obviously improve the melt viscosity and elasticity of PLA, meanwhile the complex viscosity, the storage modulus and loss modulus also increase with increasing the concentration of CP/SE, which will open a wider way for expanding application of PLA material in blow-film, blow-molding, extrusion, and foaming.
3. Although PLA/CP/SE composites are a microphase separation system and the addition of CP/SE can effectively hinder the crystallization of PLA, while the tensile strength of PLA is increased.

References

1. Martin, O.; Avérous, L. Polymer 2001, 42, 6209.
2. Okada, M. Prog Polym Sci 2002, 27, 87.
3. Fang, Q.; Hanna, M. A. Ind Crop Prod 1999, 10, 47.

4. Kanebo Ltd., Japan. Available at: www.kanebotx.com; Accessed on Aug. 27, 2002.
5. Tsuji, H.; Fukui, I. Polymer 2003, 44, 2891.
6. Park, E. S.; Cho, H. C.; Kim, M. N.; Yoon, J. S. J Appl Polym Sci 2003, 90, 1802.
7. Carlson, D.; Dubois, P.; Nie, L.; Narayan, R. Polym Eng Sci 1998, 38, 311.
8. Soedergaard, A.; Niemi, M.; Selin, J. F.; Naesman, J. H. Ind Eng Chem Res 1995, 34, 1203.
9. Hitomi, M.; Yozo, K. Jpn. Pat. 10, 017, 756-A (1998).
10. Tomoyuki, N.; Koichiro, T.; Jun, T. Jpn. Pat. 2, 005, 239, 932-A (2005).
11. Simões, C. L.; Viana, J. C.; Cunha, A. M. J Appl Polym Sci 2009, 112, 345.
12. Wu, D. F.; Zhang, Y. S.; Zhang, M. Eur Polym Mater 2008, 44, 2171.
13. Ohkoshi, I.; Abe, H.; Doi, Y. Polymer 2000, 4, 5985.
14. Lu, J. M.; Qiu, Z. B.; Yang, W. T. Polymer 2007, 48, 4196.
15. Tsuji, H.; Muramatsu, H. J Appl Polym Sci 2001, 81, 2151.
16. Shirahase, T.; Komatsu, Y.; Tominaga, Y.; Asai, S.; Sumita, M. Polymer 2006, 47, 4839.
17. Sheth, M.; Kumar, R. A.; Dave, V.; Gross, R. A.; Mccarthy, S. P. J Appl Polym Sci 1997, 66, 1495.
18. Meaurio, E.; Zuza, E.; Sarasua, J. R. Macromolecules 2005, 38, 9221.
19. Jiang, L.; Wolcott, M. P.; Zhang, J. W. Biomacromolecules 2006, 7, 199.
20. Monticelli, O.; Oliva, D.; Russo, D.; Clausnitzer, C.; Pîotschke, P.; Voit, B. Macromol Mater Eng 2003, 288, 318.
21. Sudduth, R. D. Polym Eng Sci 1996, 36, 2135.
22. Sarasua, J. R.; Arraiza, A. L.; Balerdi, P.; Maiza, I. Polym Eng Sci 2005, 45, 745.
23. Sudduth, R. D. Polym Eng Sci 2003, 43, 519.
24. Mondragon, I.; Nazabal, J. J Appl Polym Sci 1986, 32, 6190.
25. Porter, R. S.; Wang, L. H. Polymer 1992, 33, 520.
26. Sultania, M.; Rai, J. S. P. Eur Polym Mater 2010, 46, 2019.
27. Wittea, F. M.; Goemansa, C. D.; van der Lindea, R. Prog Org Coat 1997, 32, 241.
28. Niu, X. F.; Feng, Q. L.; Wang, M. B.; Guo, X. D.; Zheng, Q. X. Polym Degrad Stabil 2009, 94, 176.
29. Meaurio, E.; Zuza, E.; Sarasua, J. R. Macromolecules 2005, 38, 1207.
30. Schmaljohann, D.; Pîotschke, P.; Hîa1ssler, R; Voit, B I Macromolecules 1999, 32, 6333.
31. Qi, R. R.; Jin, X.; Nie, J. H.; Yu, W.; Zhou, C. X. J Appl Polym Sci 2005, 97, 201.
32. Chopra, D.; Kontopoulou, M.; Vlassopoulos, D.; Hatzikiriakos, S. G. Rheol Acta 2002, 41, 10.
33. Inoue, T. Prog Polym Sci 1995, 20, 119.
34. Chen, W. J; Li, X. L.; Dong, T.; Jiang, M. Macromol Chem Phys 1998, 199, 327.